



A Mine Ventilation System Energy Saving Technique Based on an Improved Equilibrium Optimizer

Bao-cai Yu* and Liang-shan Shao

Institute of Systems Engineering, Liaoning Technical University, Fuxin, China

OPEN ACCESS

Edited by:

Ali Bassam,
Universidad Autónoma de Yucatán,
Mexico

Reviewed by:

Jingbo Wang,
Kunming University of Science and
Technology, China
Ramin Ranjbarzadeh,
Dublin City University, Ireland
Ismail Altin,
Karadeniz Technical University, Turkey

*Correspondence:

Bao-cai Yu
1378425366@qq.com

Specialty section:

This article was submitted to
Process and Energy Systems
Engineering,
a section of the journal
Frontiers in Energy Research

Received: 08 April 2022

Accepted: 31 May 2022

Published: 11 August 2022

Citation:

Yu B-c and Shao L-s (2022) A Mine
Ventilation System Energy Saving
Technique Based on an Improved
Equilibrium Optimizer.
Front. Energy Res. 10:913817.
doi: 10.3389/fenrg.2022.913817

Over the years, the ventilation systems used in coal mines have become more and more complex. Due to a lack of scientific and effective management, the energy consumed by ventilation systems has rapidly increased, resulting in considerable wasted energy. To solve this problem, the authors established a nonlinear optimization model aimed at minimizing the total energy consumption of a mine ventilation network. Furthermore, the authors propose an improved equilibrium optimizer algorithm to solve the model. First, the population is initialized by a chaotic map. Second, the adjustment strategy of a trigonometric function is introduced to improve the index F , which improves the global development ability of the algorithm, avoids falling into local optimum, and can improve the local search ability in the later stages. Then, Gaussian disturbance is introduced to enhance the diversity of particles and avoid falling into the local optimum. Finally, a learning factor was introduced to improve the generation rate G and improve the algorithm's integrity; it was then compared with other algorithms. The simulation results show that the performance of the improved algorithm is significantly better than other algorithms. It was tested with the ventilation system of Wangjialing mine of Zhongmei Huajin Energy Co., Ltd. The results showed that the energy consumption of the ventilation system was reduced by 17.83%. This method can save the mine about 2 million yuan RMB every year. The economic effect is remarkable, we achieved the purpose of energy conservation and emission reduction, and the effectiveness of the proposed method was verified.

Keywords: ventilation energy consumption, equilibrium optimizer algorithm, ventilation network optimization, Gaussian disturbance, energy saving and emission reduction

1 INTRODUCTION

A mine's ventilation system is one of the most essential coal mine safety production systems. Energy consumed by the ventilation system accounts for about one third of the total energy consumption of a coal mine. Over the years, ventilation systems have become more and more complex. Due to the poor planning of mine ventilation systems and a lack of scientific and effective management, there is considerable waste of energy as well as potential safety hazards. To ensure safe production in a mine, improve mine ventilation conditions, and reduce energy waste, ventilation systems must be optimized (Shao et al., 2020; Su and Ouyang, 2021). Ventilation system optimization is a hot topic of research in this field (Wang et al., 2019).

Mine ventilation systems are highly coupled and complex systems. Traditional methods are not only slow to solve the problem but also poor at solving the problem, so we must use new methods to

solve this problem. With the ongoing development of intelligent algorithms, many scholars have introduced intelligent algorithms to optimize mine ventilation systems. Liangshan Shao et al. optimized the problem based on simulated annealing and improved the particle swarm optimization algorithm, thus reducing the energy consumed for ventilation by 25.3% (Shao et al., 2021). Xingguo Zhang et al. studied a ventilation network solution based on an ACPSO algorithm, and the air quantity optimization scheme obtained had the minimum total ventilation energy consumption (Zhang and Zhou, 2018). Zhong et al. proposed an efficient mine ventilation solution method based on minimum independent closed loops to effectively optimize the mine ventilation system (Zhong et al., 2020). Yixin Su used the improved genetic algorithm to search the optimal weight and threshold of the network globally, and used BP algorithm to conduct local optimization, and finally obtained the wind speed prediction value (Su et al., 2017). Xinzhong Wu in fireworks algorithm to join the elite reverse learning strategy, strengthen the search algorithm in the field of space, Thus improve the global searchability (Wu et al., 2019).

The above methods have some limitations for solving the nonlinear optimization model of mine ventilation systems. For example, the algorithm has many parameters and this can easily result in local optimization, so the algorithm must be improved. The equilibrium optimizer (EO) is a physics-based meta-heuristic algorithm, proposed by Faramarzi et al., in 2019 (Faramarzi et al., 2020a). Compared with the genetic algorithm (Li et al., 2007), which can easily result in local optimization and has low execution efficiency, the particle swarm optimization (PSO) algorithm (Marini and Walczak, 2015) with premature phenomenon and the ant colony algorithm (Dorigo et al., 2006) which is easy to appear algorithm stagnation, it has the advantages of fewer parameters, high execution efficiency, and outstanding global optimization ability. Therefore, it has been successfully applied to multi-objective optimization (Abdel-Basset et al., 2020), photovoltaic cell parameter optimization (Dinh, 2021), multimodal medical image fusion (Wang et al., 2021), feature selection (Wang et al., 2021), and other fields.

Many experts and scholars have developed improvements to the performance of the equalization optimizer algorithm. Sayed et al. constructed a stable search mechanism by introducing chaotic mapping to improve the feature selection efficiency of the algorithm (Sayed et al., 2020). Fan et al. improved the optimization accuracy of the algorithm through reverse learning and a new concentration update formula (Fan et al., 2021). Dinkar et al. (2021) updated the candidate solution concentration using the random walk of Laplace distribution and then accelerated the development by reverse learning to make the algorithm converge rapidly. However, these improved methods have only improved parts of the equalization optimizer algorithm. To apply the EO algorithm to mine ventilation system optimization, the algorithm must be comprehensively improved. We propose an improved equalization optimizer (IEO) algorithm combined with chaotic mapping, trigonometric function, Gaussian disturbance, and a learning factor, and compare it with other algorithms to verify the ability of the IEO algorithm to optimize mine ventilation systems.

The main contributions of this paper include:

- Establishing a nonlinear optimization model aimed at minimizing the total energy consumption of a mine ventilation network to address the problem of mine ventilation optimization.
- Proposing an IEO algorithm based on chaotic mapping, trigonometric function, Gaussian disturbance, and a learning factor.
- The performance of the proposed IEO algorithm is validated against seven unimodal benchmark functions, six multimodal benchmark functions, and three fixed-dimension multimodal benchmark functions.

- Performance comparisons between the proposed IEO and other state-of-the-art algorithms using various performance metrics for the optimization of the ventilation system of Wangjialing mine, belonging to Zhongmei Huajin Energy Co., Ltd.

The remainder of the paper is organized as follows: **Section 2** establishes the mine ventilation network model. **Section 3** introduces the EO algorithm. **Section 4** describes the IEO algorithm. **Section 5** tests the IEO algorithm's performance. **Section 6** describes the engineering application analysis. **Section 7** gives the conclusion and the future research direction.

2 MINE VENTILATION SYSTEM MODELING

To realize the intellectualization and automation of the regulation and optimization of mine ventilation systems, a mathematical model of mine ventilation network optimization based on minimum power consumption has been established (Hao et al., 2012; Pei et al., 2017). The model constraints are as follows:

- (1) The mine ventilation network follows the node air quantity balance law (Wei, 2011). That is, the air quantity flowing into a node is equal to the air quantity flowing out. This can be described as:

$$\sum_{j=1}^{N_i} \omega_{ij} Q_i = 0, (N_i = 1, 2, \dots, J) \quad (1)$$

$$\omega_{ij} = \begin{cases} 1 & \text{branch } i \text{ flows into node } j \\ 0 & \text{the } j \text{ node is not the endpoint of the } i \text{ branch} \\ -1 & \text{branch } i \text{ flows out node } j \end{cases} \quad (2)$$

Where, N_i is the total number of branches with node j as the endpoint of the mine, with node j as the endpoint. Q_i represents the quantity of air in this branch i , unit m^3/s . J is the total number of ventilation network nodes.

- (2) A mine ventilation network follows the loop resistance balance law (Oliveira et al., 2015). That is, the algebraic sum of resistance, natural wind pressure, and mechanical wind pressure of each branch in the M ($M = (N - J + 1)$)

loop is zero, and N is the total number of branches. This can be described as:

$$\sum_{i=1}^M c_{ij} (R_i Q_i^2 - (P_i + F_i Q_i)) = 0, \tag{3}$$

$$c_{ij} = \begin{cases} 1 & i \in l, \text{ the } i \text{ branch is in the same direction as the loop} \\ 0 & i \notin l \\ -1 & i \in l, \text{ the } i \text{ branch is opposite to its loop} \end{cases} \tag{4}$$

Where P_i is the natural wind pressure of branch i , unit Pa, $F_i Q_i$ is the mechanical wind pressure of branch i , unit Pa, and R_i is the resistance of branch i , unit $N \cdot s^2 \cdot m^{-8}$.

(3) To make the fan work stably and avoid surge (Dong and Li, 2008), it is generally stipulated that the upper limit of the actual working wind pressure of the fan shall not exceed 90% of its maximum wind pressure, and the lower efficiency limit shall not be less than 60%. This can be described as:

$$H \leq 0.9H_{\max} \tag{5}$$

$$\eta \geq 60\% \tag{6}$$

Where H_i represents the operating pressure of the fan and η represents the efficiency of the fan.

(4) Finally, according to the «The Coal Mine Safety Rules» and the actual situation of the mine, the lower and upper limits of the regulated air quantity and air pressure of the adjustable branches can be calculated. This can be described as:

$$H_{i\min} \leq H_i \leq H_{i\max} \tag{7}$$

$$Q_{i\min} \leq Q_i \leq Q_{i\max} \tag{8}$$

where $Q_{i\min}$ and $Q_{i\max}$, respectively, represent the lower limit and upper limit of the adjustable branch air quantity, unit m^3/s . $H_{i\min}$ and $H_{i\max}$ represent the lower limit and upper limit, respectively, of the regulated wind pressure of the branch, unit Pa.

On the premise of meeting the demand air distribution, the minimum total power of the fan is regarded in the ventilation network as the optimization goal of the model. This can be described as:

$$\min f = \sum_{i=1}^n H_{Fi} Q_i \tag{9}$$

where H_{Fi} represents the pressure of fan on branch i .

It is known that the model is a non-convex nonlinear constrained optimization problem. To better apply an intelligent algorithm to solve the problem, the penalty function was used to transform the inequality constraints: it was constructed the objective function and constraints into an augmented objective function with parameters (Jia et al., 2011) and transform the problem into an unconstrained nonlinear programming problem for solution. The augmented objective function consists of two parts: the objective function of the original problem and the penalty term constructed by the constraint function. The function of the penalty term is to restrict illegal points or data. Therefore, the upper and lower limits of adjustable air volume and wind pressure of some branches are

known, so the internal penalty function method is adopted to ensure the feasibility of the iteration points. After the above conversion, the objective function is:

$$W = \sum_{i=1}^M |H_i| |Q_i| + \iota \sum_{i=1}^L \left| \sum_{j=1}^D \omega_{ij} Q_i \right| + \kappa \sum_{i=1}^L \sum_{j=1}^N c_{ij} R_j Q_j^2 - \sum_{j=1}^N [P_j + F_j Q_j] \left| \sum_{i=1}^D \ln(\min\{0, (Q_{i\max} - Q_i)\}) + \ln(\min\{0, (Q_i - Q_{i\min})\}) \right| + \rho \sum_{i=1}^D \left| \ln(\min\{0, (H_{i\max} - H_i)\}) + \ln(\min\{0, (H_i - H_{i\min})\}) \right| + \xi \sum_{i=1}^D \left| \ln(\min\{0, (0.9H_{i\max} - H_i)\}) + \ln(\min\{0, (\eta_i - 0.6)\}) \right| \tag{10}$$

where $\iota, \kappa, \rho, \xi, \tau$ are penalty coefficients.

3 PRINCIPLE OF THE EQUALIZATION OPTIMIZER ALGORITHM

The equalization optimizer algorithm is a new physics-based algorithm for solving continuous optimization problems. The advantage of the equalization optimizer algorithm is that the solution can be changed randomly according to high exploration and exploitation. The particle concentration of the equalization optimizer is similar to the particle and position of the PSO algorithm, which represents the search agent. The search agent randomly updates their concentration and names it the equilibrium candidate solution with the best self searched. Finally, it reaches the equilibrium state, when it can be divided into three stages: population initialization, equilibrium pool, and concentration update.

3.1 Inspiration

The EO algorithm was inspired by the physical mass balance equation, which provides the physical basis by controlling the controller's volume weight input quality, output quality, and production quality. A section of the breeze equation represents the general mass balance equation, in which the change of mass over time is equal to the mass entering the system minus the mass leaving the system plus the original mass. This is described in Eq. 11.

$$C = C_{eq} + (C_0 - C_{eq})F + \frac{G}{\lambda V} (1 - F) \tag{11}$$

In the equation, C represents the current particle concentration, C_{eq} represents the concentration when the particles in the control product are in equilibrium without iteration, C_0 is the original concentration of the particles, G represents the mass generation rate in the control product, λ is a random number between $[0,1]$, V is a unit volume, and F index to balance development and exploration.

3.2 Equilibrium Pool and Its Candidate Solution

The equilibrium state is the final convergence state of the algorithm and is globally optimal. The EO algorithm

constructs a vector called the equilibrium pool, which provides equalization candidate particles. Through experiments, it can be determined in five candidate solutions in the equilibrium pool, four of which are the best particles identified in the whole optimization process. The other is the mathematical average of the other four. The four best particles are helpful to explore the search space, and the average is helpful for exploitation. The equilibrium pool vector can be described as shown in Eq. 12:

$$\vec{C}_{eq,pool} = \left\{ \vec{C}_{eq(1)}, \vec{C}_{eq(2)}, \vec{C}_{eq(3)}, \vec{C}_{eq(4)}, \vec{C}_{eq(ave)} \right\} \quad (12)$$

where $\vec{C}_{eq,pool}$ is the candidate solution selected with the same probability in the equilibrium pool.

3.3 F Index

Index F plays a significant role in the exploration and exploitation phases of the balanced EO algorithm. The calculation is described in Eq. 13:

$$F = e^{(-\lambda(t-t_0))} \quad (13)$$

where λ is a random vector between $[0,1]$. t is an iterative function; as the number of iterations decreases, the equation is shown in Eq. 14:

$$t = \left(1 - \frac{Iter}{Max_iter} \right)^{\alpha_2 \frac{Iter}{Max_iter}} \quad (14)$$

where $Iter$ and Max_iter represent the current and maximum iteration times, respectively. The calculation of t_0 is described in Eq. 15:

$$\vec{t}_0 = \frac{1}{\lambda} \ln \left(-\alpha_1 \text{sign}(\vec{r} - 0.5) [1 - e^{-\lambda t}] \right) + t \quad (15)$$

In the formula, α_1 and α_2 are constants used to control the exploration and exploitation abilities. The higher the value of α_1 , the stronger the exploration ability and the weaker the exploitation ability. The higher the value of α_2 , the stronger the exploitation ability and the weaker the exploration ability. Therefore, we can write the index F as (Eq. 16):

$$\vec{F} = \alpha_1 \text{sign}(\vec{r} - 0.5) \left[e^{-\lambda t} - 1 \right] \quad (16)$$

3.4 Generation Rate

The generation rate G enables the EO algorithm to provide accurate solutions by improving the exploitation stage. The generation rate is defined by the first-order exponential decay rate, as shown in Eq. 17:

$$\vec{G} = \vec{G}_0 e^{-\vec{k}(t-t_0)} \quad (17)$$

where \vec{G}_0 is the initial value and k is an attenuation constant equal to λ , so the final expression of the generation rate is described in Eq. 18:

$$\vec{G} = \vec{G}_0 e^{-\vec{k}(t-t_0)} = \vec{G}_0 \vec{F} \quad (18)$$

where:

$$\vec{G}_0 = \overrightarrow{GCP} (\vec{C}_{eq} - \vec{\lambda} \vec{C}) \quad (19)$$

$$\overrightarrow{GCP} = \begin{cases} 0.5r_1, & r_2 \geq GP \\ 0, & r_2 < GP \end{cases} \quad (20)$$

where r_1 and r_2 neutralization is a random number between $[0,1]$. GCP represents the probability that generation contributes to the update process, called the generation rate control parameter. The exceptional contribution of this probability is that many examples use this generation term to update their state. GCP can be obtained from Eq. 20. GP ($GP = 0.5$), the generic possibility, can achieve a good balance between development and exploration. The final update of the EO algorithm is shown in Eq. 21:

$$\vec{C} = \vec{C}_{eq} + (\vec{C}_0 - \vec{C}_{eq}) \vec{F} + \frac{\vec{G}}{\lambda V} (1 - \vec{F}) \quad (21)$$

4 IMPROVED EQUALIZATION OPTIMIZER ALGORITHM

4.1 Chaotic Map Initialization Population

The ergodicity and randomness of chaotic mapping sequences are widely used to optimize search problems. To improve the individual diversity and make the initial particles as evenly distributed in the search space as possible, this paper uses cat mapping, because the cat mapping structure is simple and it is not easy to fall into short cycles and periodic fixed points (Peterson, 2020) to generate the initial population. The expression of cat mapping is shown in Eq. 22:

$$\begin{bmatrix} x_{i+1} \\ y_{i+1} \end{bmatrix} = \begin{bmatrix} b_1 & b_2 \\ b_3 & b_4 \end{bmatrix} \begin{bmatrix} x_i \\ y_i \end{bmatrix} \text{mod}1 \quad (22)$$

where, b_1, b_2, b_3 and b_4 is the mapping coefficient, (they are positive integer), satisfying the relationship in Eq. 23, x_{i+1} and y_{i+1} are the coordinates after mapping, and mod1 is the coordinate before mapping, indicating the decimal part of the mapping coefficient.

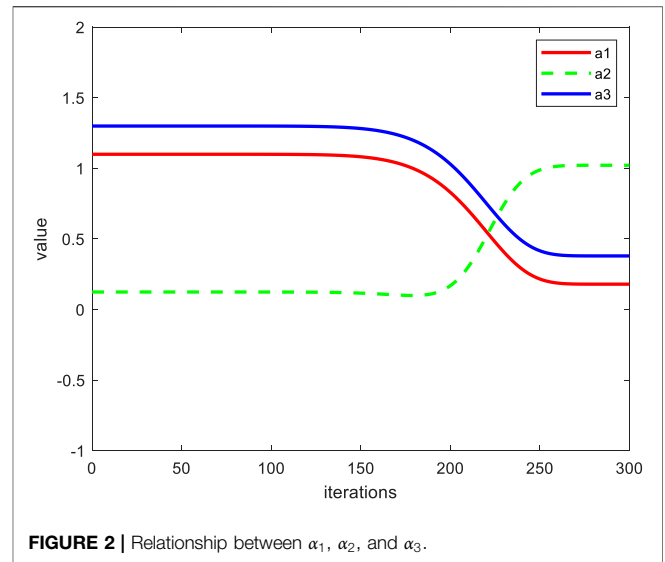
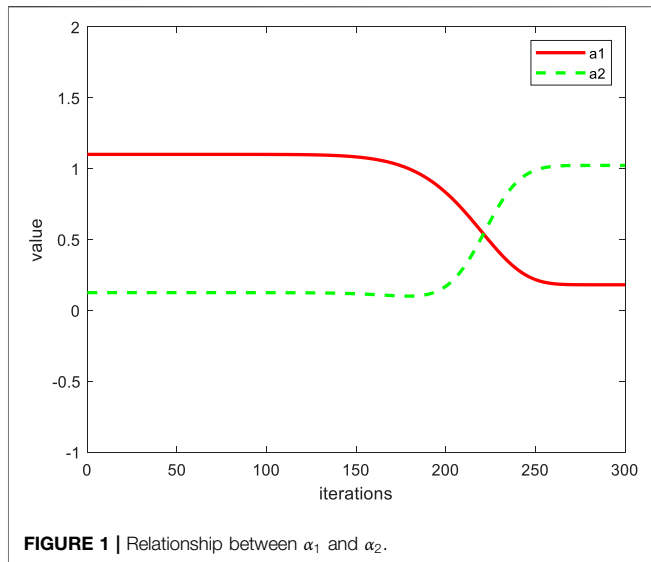
$$b_1 b_4 - b_2 b_3 = 1 \quad (23)$$

The initial population generated by cat chaotic mapping can be expressed as shown in Eq. 24:

$$C' = [c'_{i1}, c'_{i2}, \dots, c'_{id}] \quad (24)$$

4.2 Improvement Index

In the equilibrium optimization algorithm, the index F plays a very important role in the exploration and exploitation phases of the algorithm. α_1 and α_2 control the exploration and development ability. The higher the value of α_1 , the stronger the exploration ability and the weaker the exploitation ability. The higher the value of α_2 , the



stronger the exploitation ability and the weaker the exploration ability. In the standard EO algorithm, two parameters are definite value. Therefore, the algorithm cannot adaptively adjust the exploration and exploitation ability according to the iteration, and there will be unstable optimization. At the beginning of optimization a larger value is set, and the value of α_1 is gradually reduced. Setting a smaller value and gradually increasing the value of α_2 improves the algorithm’s global development ability, avoids falling into local optimization, and improves the local search ability in the later stages. Therefore, using the adjustment strategy of introducing a trigonometric function, the parameters α_1 and α_2 are improved. The improved parameters are shown in Eqs 25–26.

$$\alpha_1 = a + (b - a) * e^{\left[-20 + \left(\frac{t}{T_{\max}} \right)^{10} \right]} + 0.1 \quad (25)$$

$$\alpha_2 = c + d * \cos(\alpha_1 * \pi) \quad (26)$$

where a, b, c, and d are constants.

Figure 1 shows the change curves of α_1 and α_2 . It can be seen that when the number of iterations is less than 170, the values of α_1 and α_2 are relatively flat, which can improve the global search speed. When the number of iterations is more than 170 and less than 240, the value of α_1 and α_2 change significantly, which can make the particle concentration close to the optimal equilibrium concentration. When the number of iterations is more than 240 and less than 300, the α_1 and α_2 values become flat again, which ensures the accuracy of the local search. At the same time, the two can restrict each other to ensure the early search speed and avoid falling into local optimization to balance the exploration and exploitation abilities.

4.3 Gaussian Perturbation

Considering that the five candidate solutions in the equilibrium pool constructed by the standard EO algorithm

represent the best equilibrium concentration, there is still an ample change space. To avoid falling into local optimization and increase particle diversity, the four best particles are slightly Gaussian perturbed (Gleiser and Dotti, 2005) to improve the algorithm’s ability to explore the optimal value. The expression is:

$$\vec{C}_{eq(i)}^g = \vec{C}_{eq(i)} (1 + \text{Gaussian}(\mu, \sigma^2)) \quad i = 1, 2, 3, 4 \quad (27)$$

$$\vec{C}_{eq,pool}^g = \begin{cases} \vec{C}_{eq,pool}^g & f(\vec{C}_{eq,pool}^g) < f(\vec{C}_{eq,pool}) \\ \vec{C}_{eq,pool} & \text{others} \end{cases} \quad (28)$$

where $\vec{C}_{eq(i)}^g$ is the concentration of four particles in the equilibrium pool after disturbance; Gaussian(\bullet) is the Gaussian function, μ is the mean, σ is the variance; $\vec{C}_{eq,pool}^g$ is the equilibrium pool after disturbance, and $f(\bullet)$ is the fitness function. Through the small Gaussian perturbation of $\vec{C}_{eq(i)}$, the algorithm can jump out of the local optimal value, which can effectively improve the utilization and accuracy of the algorithm.

4.4 Improvement Generation Rate

The generation rate G enables the EO algorithm to provide accurate solutions by improving the development stage. In the standard EO algorithm, the first-order exponential decay rate is used to define the generation rate, and a learning factor α_3 is introduced in the concentration change stage. Its expression is shown in Eq. 29. Through α_3 we can increase the smoothness of the optimization. Through cooperation with α_1 and α_2 we can increase the algorithm’s integrity. The relationship between α_1 , α_2 , and α_3 is shown in Figure 2.

$$\alpha_3 = e + f * \cos\left(\arccos\left(\frac{\alpha_3 - c}{d}\right)\right) \quad (29)$$

TABLE 1 | Algorithm names and parameter settings.

Full name of algorithm	Abbreviation	Parameter setting
Marine predators algorithm	MPA Faramarzi et al. (2020b)	FADs = 0.2, p = 0.5
Sine cosine algorithm	SCA Mirjalili, (2016)	a = 2
Particle swarm optimization	PSO Poli et al. (2007)	w = 0.7298; c1 = c2 = 1.4962
Tunicate swarm algorithm	TSA Kaur et al. (2020)	—
Equilibrium optimization	EO Faramarzi et al. (2020a)	a1 = 2, a2 = 1, GP = 0.5
Improved equilibrium optimization	IEO	a = 0.08, b = 1, c = 0.6, d = 0.5, e = 0.8, f = 0.5

TABLE 2 | Benchmark function.

Function	Dim	Range	F _{min}
$F_1(x) = \sum_{i=1}^n x_i^2$	30	[-100,100]	0
$F_2(x) = \sum_{k=1}^n x_k + \prod_{k=1}^n x_k $	30	[-10,10]	0
$F_3(x) = \sum_{i=1}^n (\sum_{j=1}^i x_j)^2$	30	[-100,100]	0
$F_4(x) = \max_i \{ x_i , 1 \leq i \leq n\}$	30	[-100,100]	0
$F_5 = \sum_{i=1}^{n-1} [100(x_{i+1} - x_i^2)^2 + (x_i - 1)^2]$	30	[-30,30]	0
$F_6(x) = \sum_{i=1}^n ([x_i + 0.5])^2$	30	[-100,100]	0
$F_7(x) = \sum_{i=1}^n x_i^4 + \text{random}[0, 1]$	30	[-1.28,1.28]	0
$F_8(x) = \sum_{i=1}^n -x_i \sin(\sqrt{ x_i })$	30	[-500,500]	0
$F_9(x) = \sum_{i=1}^n [x_i^2 - 10 \cos(2\pi x_i) + 10]$	30	[-1.25,1.25]	0
$F_{10}(x) = -20 \exp \left\{ -0.2 \sqrt{\frac{1}{n} \sum_{i=1}^n x_i^2} \right\} - \exp \left(\frac{1}{n} \sum_{i=1}^n \cos(2\pi x_i) \right) + 20 + e$	30	[-32,32]	0
$F_{11}(x) = \frac{1}{4000} \sum_{i=1}^n x_i^2 - \prod_{i=1}^n \cos\left(\frac{x_i}{\sqrt{i}}\right) + 1$	30	[-600,600]	0
$F_{12}(x) = \frac{\pi}{n} \{10 \sin(\pi y_1) + \sum_{i=1}^{n-1} (y_i - 1)^2 [1 + 10 \sin^2(\pi y_{i+1})] + (y_n - 1)^2\} + \sum_{i=1}^n u(x_i, 10, 100, 4)$ $y_i = 1 + \frac{x_i+1}{4} u(x, a, k, m) = \begin{cases} k(x, -a)^m & x_i > a \\ 0 & -a < x_i < a \\ k(-x, -a)^m & x_i < -a \end{cases}$	30	[-50,50]	0
$F_{13}(x) = 0.1 \{ \sin^2(3\pi x_1) + \sum_{i=1}^n (x_i - 1)^2 [1 + \sin^2(3\pi i)] + (x_n - 1)^2 [1 + \sin^2(2\pi x_n)] \} + \sum_{i=1}^n u(x_i, 5, 100, 4)$	30	[-50,50]	0
$F_{14}(x) = (+\frac{1}{500} + \sum_{j=1}^{25} \frac{1}{j+\sum_{i=1}^j (x_i - a_i)}) - 1$	2	[-65,65]	1
$F_{15}(x) = \sum_{i=1}^{11} [a_i - \frac{x_i (b_i^2 + b_i x_i)}{(b_i^2 + b_i x_i + x_i^2)}]^2$	4	[-5,5]	0.00030
$F_{16}(x) = 4x_1^2 + 2.1x_1^4 + \frac{1}{3}x_1^6 + x_1x_2 - 4x_2^2 + 4x_2^4$	2	[-5,5]	-1.0316

where e and f are constants and, as the number of iterations increases, the learning factor gradually decreases, which increases the optimization accuracy in the later stage of the algorithm. Therefore, Eq. 21 is improved to Eq. 30:

$$\vec{C}' = \vec{C}_{eq}^g + \left(\vec{C}_0 - \vec{C}_{eq}^g \right) \vec{F} + \frac{\alpha_3 \vec{G}}{\lambda V} \left(1 - \vec{F} \right) \quad (30)$$

5 SIMULATION EXPERIMENT AND ANALYSIS

5.1 Experiment-Related Settings

The experimental environment was a Windows 10, 64-bit operating system, the CPU was an Intel Core i9-11950h, the main frequency was 5.0 GHz, and the memory was 16 GB.

TABLE 3 | Experimental comparison results.

F		MPA	SCA	PSO	TSA	EO	IEO
F ₁	Avg	4.7445E+00	3.1894E-07	1.5165E-06	8.8952E-20	4.3219E+00	5.6668E-44
	Std	2.8718E+01	1.2919E-07	1.9585E-06	5.9106E-20	1.0161E+01	3.8395E-43
F ₂	Avg	2.3510E-01	1.9826E-04	1.5670E+00	2.4537E-12	1.8211E+01	5.3338E-24
	Std	1.8730E-01	1.8929E-04	1.4412E+00	1.4582E-12	9.8341E+00	5.1264E-23
F ₃	Avg	3.9062E+02	2.5508E-05	1.7820E+02	5.3122E-04	1.1335E+03	2.3566E-25
	Std	5.1273E+02	3.3652E-06	9.6656E+02	1.2320E-03	6.5789E+03	8.5664E-24
F ₄	Avg	7.5089E+00	2.5103E-03	1.0829E+01	3.4255E-01	4.5534E+00	0.0000E+00
	Std	4.2117E+00	5.5788E-04	3.0867E+00	4.5735E-01	1.2190E+00	0.0000E+00
F ₅	Avg	3.8267E+01	2.1045E+01	5.4418E+02	2.1558E+02	5.6236E+03	2.8849E+00
	Std	4.1821E+01	1.2110E-01	2.2959E+03	4.8350E+00	6.2007E+02	1.5555E+01
F ₆	Avg	3.2623E+00	2.1784E+00	5.6368E-07	3.7115E+01	6.2147E+01	1.5200E-02
	Std	9.6180E+00	1.3530E-01	8.8301E-07	8.8560E-01	1.3183E+01	1.1010E-01
F ₇	Avg	5.4020E-01	2.0166E+00	1.9320E-01	1.2500E-03	4.6550E-01	2.3000E-04
	Std	4.4040E-01	5.3780E-01	5.8900E-02	3.2000E-02	2.4150E-01	5.6000E-04
F ₈	Avg	-1.0784E+03	-5.1790E+02	-8.2344E+03	-6.0703E+02	-5.6571E+03	-9.0247E+01
	Std	4.2453E+02	2.5113E+02	7.5517E+02	9.8836E+02	5.3369E+02	6.5132E+01
F ₉	Avg	6.1249E+00	3.4945E-05	5.6287E+01	5.6795E+02	6.7198E+01	5.8694E-08
	Std	3.2154E+00	2.8164E-06	1.5620E+01	1.6312E+02	8.2325E+00	1.2473E-08
F ₁₀	Avg	6.7870E-01	1.8674E-04	2.3457E+00	2.1101E+00	1.8670E+01	2.5387E-15
	Std	8.1360E-01	2.3538E-05	7.5820E-01	1.6599E+00	6.3013E+01	5.8652E-15
F ₁₁	Avg	1.3159E+00	7.2287E-06	3.8200E-02	2.2680E-01	8.2657E+00	0.0000E+00
	Std	1.5370E-01	1.3813E-06	1.6100E-02	3.3830E-01	3.7816E+00	0.0000E+00
F ₁₂	Avg	6.5100E-02	7.5160E-01	6.5805E+00	6.1361E+00	4.5679E+00	2.5600E-02
	Std	1.8600E-02	2.5480E-01	3.4634E+00	4.5975E+00	2.1132E+00	5.6800E-02
F ₁₃	Avg	3.2800E-01	2.7776E+00	1.4521E+01	1.8879E+00	2.7848E+02	1.3400E-02
	Std	3.9200E-02	1.3600E-02	1.3158E+01	1.6815E+00	8.4141E+01	2.1400E-02
F ₁₄	Avg	1.1600E-01	1.0200E+00	1.1800E-01	1.2200E-01	1.0050E-01	1.1080E-01
	Std	6.6285E-02	5.5623E-04	1.1125E-02	7.6250E-03	2.9890E-05	3.2516E-15
F ₁₅	Avg	3.1200E-03	3.1500E-03	3.3000E-03	3.9800E-03	3.0500E-03	3.0000E-04
	Std	4.5680E-02	5.2500E-03	6.6200E-04	3.3500E-03	1.2500E-05	2.5600E-06
F ₁₆	Avg	-1.0300E+00	-1.0298E+00	-1.0314E+00	-1.0313E+00	-1.0315E+00	-1.0316E+00
	Std	5.2360E-06	4.2980E-05	1.2350E-05	2.2250E-06	5.6800E-04	3.1560E-07

The best results are shown in bold text. The best results means the closer the value of std and avg is to 0, the better the algorithm solving ability is.

The algorithm program was written based on Matlab 2020b. **Table 1** shows the full names and abbreviations of the algorithms and their parameter settings.

Simulation experiments were carried out on 13 benchmark functions. **Table 2** shows the details of the test functions. Among them, functions F₁–F₇ are unimodal benchmark functions, and there is only one global optimal meridian, used to evaluate the convergence speed of the algorithm. Functions F₈–F₁₃ are multimodal benchmark functions used to evaluate the algorithm’s performance in avoiding local optimization and exploration. Functions F₁₄–F₁₆ are fixed-dimension multimodal benchmark functions.

5.2 Experimental Results and Analysis

To prove the effectiveness and robustness of the proposed IEO, the IEO algorithm was compared with the MPA, SCA, PSO, TSA, and EO algorithms. The population number of all algorithms was 30, and the maximum number of iterations was 500. All algorithms were run independently on 13 benchmark functions, 50 times, and the average and standard deviation of these 50 times was taken as the final evaluation index. **Table 3** shows the specific experimental data, where Avg represents the average optimal fitness value and Std

represents the standard deviation; the best results are shown in bold text.

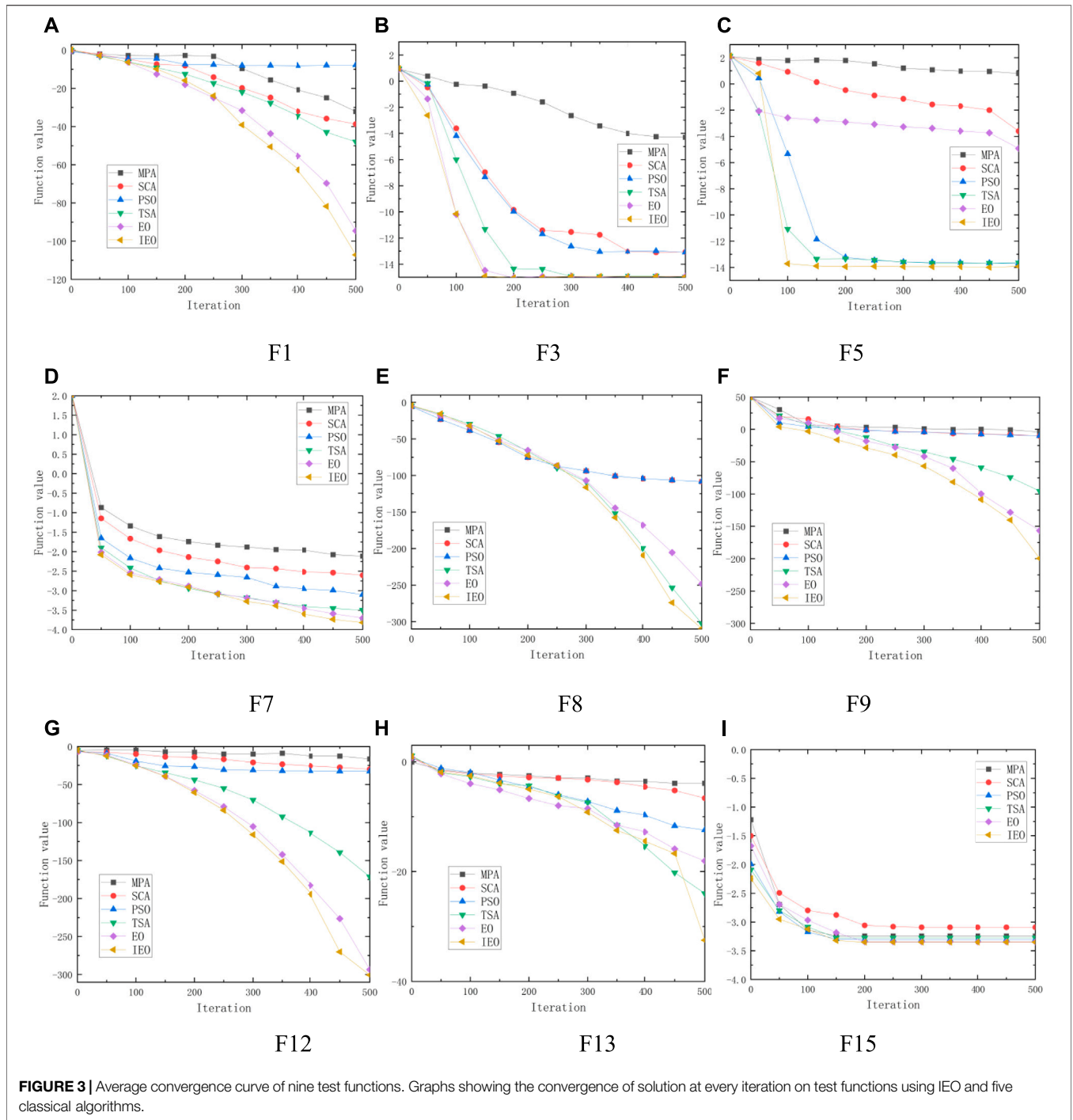
According to **Table 4**, in the unimodal function, the proposed IEO algorithm is better than the other algorithms because of the introduction of parameters α_1 , α_2 , and α_3 . It improves the integrity of the algorithm. It balances the optimization performance well in terms of exploration and exploitation. In the multimodal function, the performance of the proposed IEO algorithm is also better than the other algorithms, because the introduction of Gaussian disturbance can enhance the ability of particles to escape from local optimization.

5.3 Convergence Analysis

Figure 3 shows the convergence evaluation results of the IEO algorithm and the comparison algorithms in **Table 1** for different functions. To facilitate observation, the logarithm with base 10 was taken as the ordinate. From **Figure 3**, it can be seen that the convergence speed of the proposed IEO algorithm is faster than the other algorithms in both the exploration and exploitation stages. It shows that the three parameters introduced, α_1 , α_2 , and α_3 , can cause the algorithm to reach a dynamic equilibrium state and help the particles converge in a better direction. Furthermore, the search accuracy is better than the other algorithms. This result is inseparable from the strategy of

TABLE 4 | Air resistance quantity of some branches.

Branch number	Q $\text{m}^3 \cdot \text{s}^{-1}$	R $\text{N} \cdot \text{s}^2 \cdot \text{m}^{-8}$	Adjustable	Branch number	Q $\text{m}^3 \cdot \text{s}^{-1}$	R $\text{N} \cdot \text{s}^2 \cdot \text{m}^{-8}$	Adjustable	Branch number	Q $\text{m}^3 \cdot \text{s}^{-1}$	R $\text{N} \cdot \text{s}^2 \cdot \text{m}^{-8}$	Adjustable	Branch number	Q $\text{m}^3 \cdot \text{s}^{-1}$	R $\text{N} \cdot \text{s}^2 \cdot \text{m}^{-8}$	Adjustable
1	5.4983	0.00008936	N	23	68.0493	0.00402	N	45	2.716	0.00000831	N	67	0.3253	0.00000452	Y
2	5.4983	0.00006899	N	24	68.0493	0.00001746	N	46	33.7613	0.00006497	N	68	1.3207	0.00006467	Y
3	3.7018	0.00006706	Y	25	68.0493	0.00009132	N	47	33.7613	0.0000496	N	69	0.3466	0.00002022	Y
4	3.7018	0.00007189	Y	26	3.8702	0.00007788	N	48	58.8938	0.00008058	N	70	1.3207	0.008884	N
5	236.4348	0.00003053	N	27	1.8825	0.00006844	N	49	58.8938	0.00005265	N	71	67.8693	0.001224	N
6	236.4348	0.00005315	N	28	2.9562	0.00002784	N	50	28.0962	0.00009993	Y	72	61.3069	0.001661	N
7	236.4348	0.0000976	N	29	2.9562	0.00005758	N	51	1.7168	0.00004133	N	73	97.5121	0.003326	N
8	2.211	0.00001674	N	30	2.8893	0.00006941	N	52	29.4379	0.00009551	Y	74	85.7333	0.0168	N
9	1.9289	0.00007748	N	31	1.8943	0.00006489	N	53	1.9103	0.00002441	N	75	85.3752	0.00657	N
10	1.9289	0.00009682	N	32	1.8943	0.00009893	N	54	10.0563	0.00004614	N	76	97.3418	0.0003496	N
11	14.7881	0.07755	N	33	1.8943	0.00003318	Y	55	10.0563	0.07459	Y	77	57.5472	0.016	N
12	14.7881	0.000073	N	34	3.091	0.00004701	Y	56	1.9103	0.06913	N	78	86.985	0.001299	N
13	14.7881	0.00003508	N	35	3.091	0.00000208	N	57	2.4061	0.00216	N	79	20.5388	0.00008421	N
14	14.7881	0.00009285	N	36	18.7454	0.06289	N	58	14.6298	0.01554	N	80	57.0161	0.008713	N
15	27.0952	0.0807398	N	37	18.7454	0.196	Y	59	14.6298	0.009927	Y	81	56.5316	0.008741	N
16	2.9222	0.00003218	N	38	2.3364	0.00009302	N	60	1.4414	0.00004113	Y	82	55.7443	0.04114	N
17	24.1731	0.00003854	N	39	2.3364	0.00001179	N	61	1.3453	0.00006609	N	83	44.2401	0.00512683	N
18	24.1731	0.08833	N	40	2.3364	0.00001153	Y	62	0.962	0.00005929	Y	84	26.0291	0.15778	N
19	3.8702	0.00004987	N	41	52.2002	0.00003354	Y	63	0.962	0.00006413	Y	85	55.4608	0.0785	N
20	3.356	0.00003534	N	42	0.4844	0.00001574	N	64	6.5623	0.00005967	Y	86	56.4557	0.0015	N
21	0.5141	0.00000241	Y	43	2.716	0.00005122	N	65	1.0818	0.00006483	Y	87	122.087	0.00003188	N
22	0.5141	0.00000135	N	44	2.716	0.00002944	Y	66	0.3253	0.00001766	N	88	56.9318	0.001873	N



introducing Gaussian disturbance. **Figure 4** is a boxplot showing these algorithms on the test function. It can be seen from **Figure 4** that the degree of deviation from the optimal value found by the IEO algorithm in the process of 50 operations is much less than with the other five algorithms. It can be seen from **Table 3** that the proposed IEO algorithm has faster convergence speed and higher optimization accuracy in both unimodal and multimodal functions.

6 ENGINEERING APPLICATION ANALYSIS

6.1 Optimization Algorithm for a Mine Ventilation System Based on the Improved Equalization Optimizer Algorithm

The specific process of the mine ventilation optimization algorithm based on the IEO algorithm is as follows:

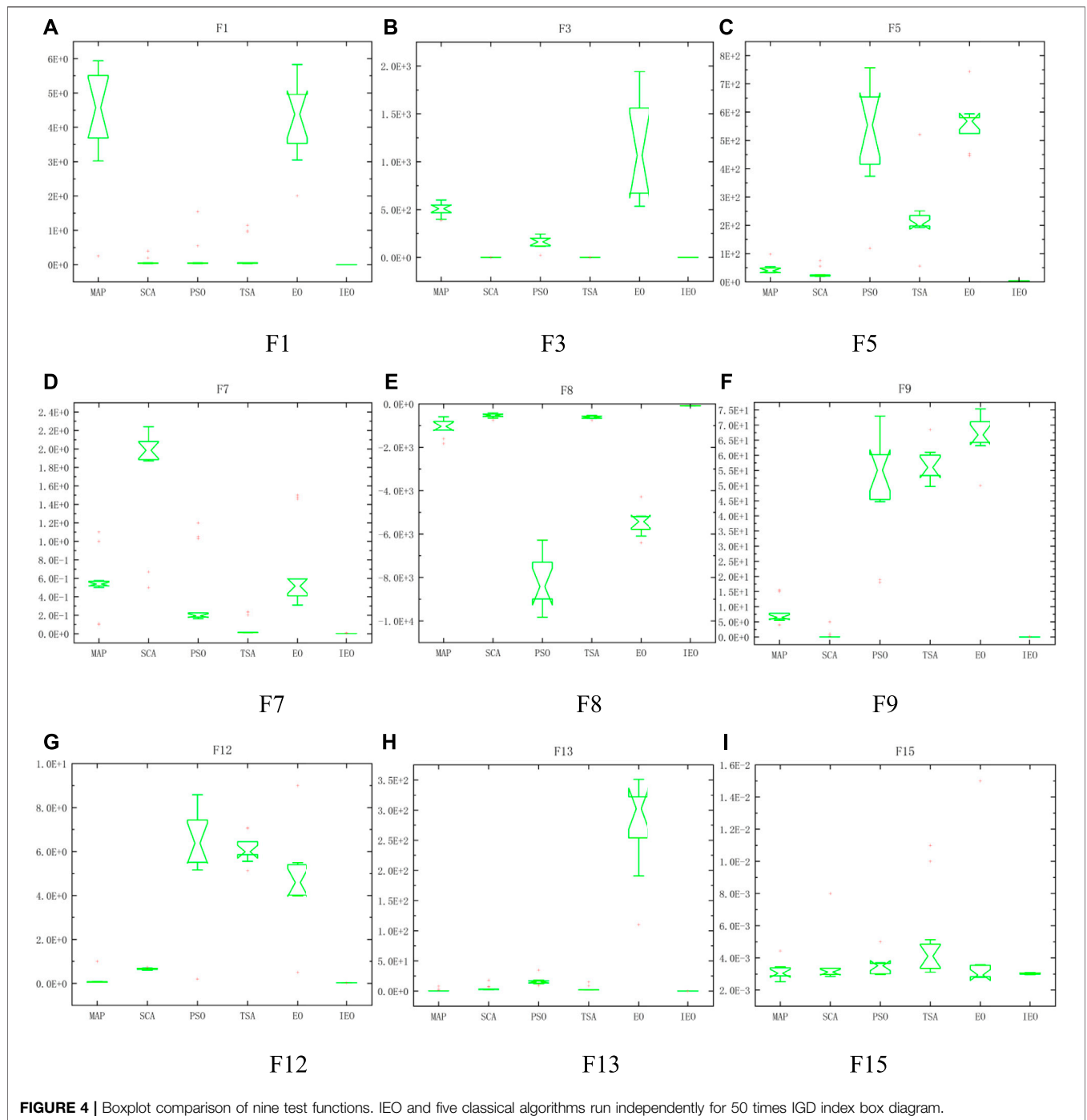


FIGURE 4 | Boxplot comparison of nine test functions. IEO and five classical algorithms run independently for 50 times IGD index box diagram.

Step 1: input population size M ; maximum iteration number T_{max} ; constants $a, b, c, d, e,$ and f ; the number of ventilation network nodes and branches; branch air quantity; and wind resistance. Each particle in the equalization optimizer represents the initial air quantity value of the branch.

Step 2: create $C_{eq1}-C_{eq4}$, four empty lists to store four candidate solutions.

Step 3: perform chaotic mapping to initialize the population and obtain a higher quality initial population.

Step 4: determine whether the current iteration number $Iter$ is less than the maximum iteration number $Maxiter$. If it is less, repeat Steps 1 to 9 until the iteration stop condition is met. Otherwise, go to Step 10.

Step 5: calculate the fitness of each particle in the population.

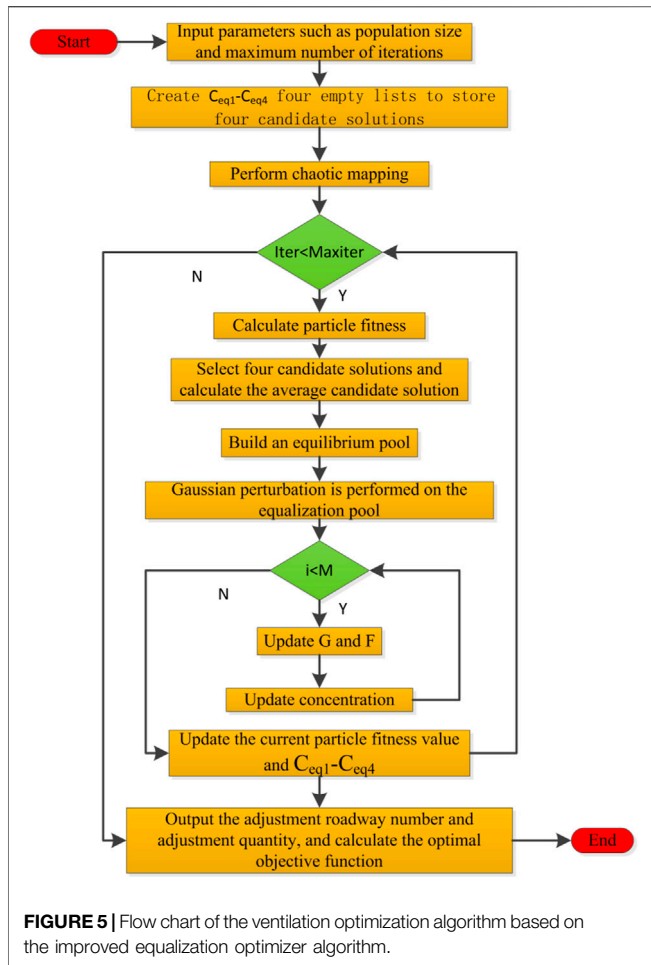


FIGURE 5 | Flow chart of the ventilation optimization algorithm based on the improved equalization optimizer algorithm.

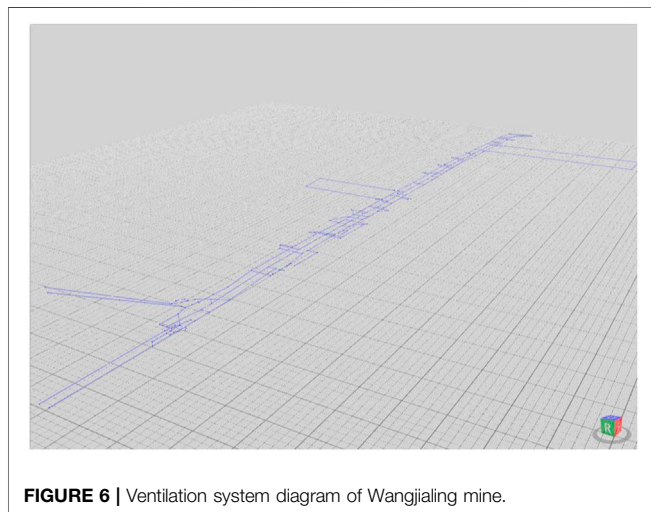


FIGURE 6 | Ventilation system diagram of Wangjialing mine.

Step 6: select four particles as candidate solutions according to the fitness of population particles, and calculate the average of the four candidate solutions as the average candidate solutions.

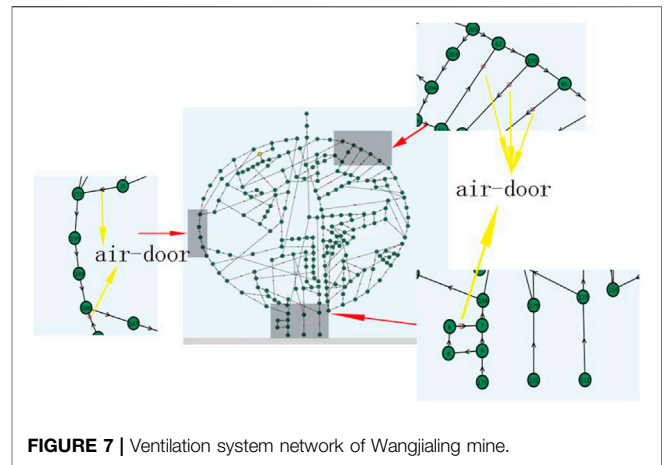


FIGURE 7 | Ventilation system network of Wangjialing mine.

Step 7: build an equilibrium pool and randomly select a candidate solution.

Step 8: perform Gaussian perturbation to perturb the particles in the equilibrium pool to further balance the algorithm's global and local search capabilities.

Step 9: enter the updating stage of individual concentration and update the particle position. If i is smaller than the population size M , update F and G with the improved formula of the trigonometric function and a section of attenuation function. Update particle positions until they meet the iteration stop conditions. Otherwise, update the current particle fitness value and the four candidate solutions.

Step 10: output the number and amount of adjusting roadway, and calculate the optimal objective function value.

Figure 5 is a flow chart showing this process.

6.2 Introduction of a Three-Dimensional Ventilation Simulation System in Wangjialing Mine

Using the Visual Studio 2019 platform, we developed three-dimensional ventilation simulation and optimization system software using C# and C++ mixed programming. The optimization method was applied to simulate Wangjialing coal mine belonging to Zhongmei Huajin Energy Co., Ltd. First measurement the resistance of the ventilation system of Wangjialing mine, then imported the measured data and the ventilation system diagram into the software, through the software we can simulated the air quantity distribution of the ventilation system in Wangjialing mine. To improve the calculation speed, simplify the mine ventilation system without affecting the results. Figure 6 shows a simplified mine ventilation system diagram. Figure 7 shows the ventilation system network diagram of Wangjialing mine. Numbering each branch and node in the diagram, the ventilation system of the mine has 213 nodes and 283 branches. Table 4 shows the basic parameters of some of the branches. See Supplementary Appendix SA for the complete data.

At present, there are three intake ventilation shafts in Wangjialing mine. The actual intake air quantities are

TABLE 5 | Comparison of the average results of 50 optimizations.

Algorithm	Original	MPA	SCA	PSO	TSA	EO	IEO
Fan power (kW)	1868	1732	1719	1725	1711	1,668	1,535
Power reduction	—	136.00	149.00	143.00	157.00	200.00	333.00
Power reduction (%)	—	7.28	7.98	7.66	8.40	10.71	17.83
Total air quantity intake (m ³ /min)	20,542	19,008	18,805	18,901	18,807	18,235	16,573
Reduced air intake quantity (m ³ /min)	—	1,534	1737	1,641	1735	2,307	3,969
Percentage reduction of total air intake (%)	—	7.47	8.46	7.99	8.45	11.23	19.32
Total air intake ratio (%)	127	118	117	118	117	113	103
Convergence algebra	—	351.25	336.78	321.58	366.12	310.55	278.34
Convergence time (min)	—	77.55	80.25	50.25	90.25	60.22	53.12

TABLE 6 | Analysis of annual cost savings.

Algorithm	Annual cost savings (yuan RMB)
MAP	863,736
SCA	946,299
PSO	908,193
TSA	997,107
EO	1,270,200
IEO	2,114,883

1286 m³ · min⁻¹, 2980 m³ · min⁻¹, and 16,089 m³ · min⁻¹. The actual air quantity demand of the mine is 16,079 m³ · min⁻¹. The return ventilation shaft has an air quantity of 20,542 m³ · min⁻¹, the ventilation resistance is 2970 Pa, the total output power of the main fan is 1868 kW, the total air quantity intake ratio is 127% in the mine, and the air intake is far greater than the actual demand, resulting in a major waste of energy.

Therefore, the method for optimizing mine ventilation systems based on the IEO algorithm proposed in this paper has been adopted by Wangjialing mine to reduce energy waste.

6.3 Analysis of Optimization Results

To verify the effectiveness of the proposed method, we compared the method with the MPA, SCA, PSO, TSA, and EO algorithms. The parameter settings were the same as those described in Section 5.1. Then, Eq. 10 was used as the particle fitness function. Each of the six algorithms was run 50 times. Table 5 shows the statistical results.

It can be seen from the Table 5 that after the six algorithms were used to optimize the ventilation system of Wangjialing mine, the IEO algorithm reduced the power used by the mine fan by 333 kW, a reduction of 17.83%, which was the most significant among the six algorithms. The intake air quantity was reduced by 3969 m³/min, a reduction of 19.32%. Compared with the other five algorithms, the IEO algorithm can effectively reduce the air quantity, and the total inlet air ratio is reduced to 103%, which greatly reduces the air quantity. The convergence algebra is 278.34 generation, which is the fastest convergence speed among the six algorithms. The convergence time was slightly slower than the PSO algorithm, but the optimization result was much better than with the PSO algorithm. Therefore, the effectiveness and timeliness of the proposed algorithm have been demonstrated. Using this method can effectively reduce the energy consumed by a mine ventilation system and achieve the purpose of energy conservation and emission reduction.

Calculated according to the standard of 0.725 yuan/kWh of power consumption costs in the industrial level period, the annual electricity costs saved after optimization of the air shaft fan using the six algorithms is shown in Table 6. This was calculated by: reduced power × 24 (h) × 0.725 yuan RMB/kWh × 365 (day). It can be seen from Table 6 that the IEO method proposed in this paper can save about 2.11 million yuan for the mine every year, making it the most cost-effective of the six algorithms.

The results of a certain operation are shown in Table 7. A negative sign indicates that the pressure value in the roadway has been reduced. In engineering applications, the corresponding roadway can be found by numbering and the resistance value of

TABLE 7 | Results of optimization of the ventilation system.

Number of branches	MPA		SCA		PSO		TSA		EO		IEO	
	Q/ m ³ · s ⁻¹	h/Pa	Q/ m ³ · s ⁻¹	h/Pa	Q/ m ³ · s ⁻¹	h/Pa	Q/ m ³ · s ⁻¹	h/Pa	Q/ m ³ · s ⁻¹	h/Pa	Q/ m ³ · s ⁻¹	h/Pa
33	1.1943	—	1.1025	—	1.0025	—	1.5623	—	0.1943	-0.12	0.2435	0.67
37	17.7454	—	15.6325	-1.10	17.6638	—	18.1064	—	17.6121	—	16.9354	—
50	26.0962	-2.05	27.0663	—	24.0258	-2.11	27.6528	—	27.0962	—	20.1312	3.05
59	13.5598	—	14.8215	—	13.6298	—	19.8528	+0.02	13.5581	—	12.8357	—
191	2.9002	—	2.8235	—	1.9352	—	2.0025	—	1.0262	-1.25	2.0652	—
199	3.5146	—	3.6521	—	3.6658	—	3.9687	—	3.8612	—	4.0052	-0.28
210	13.1215	-0.44	16.528	—	17.258	-0.55	15.2115	—	17.5512	—	16.211	—
226	1.8513	—	1.8522	—	1.8524	—	1.9000	—	1.8733	—	1.5521	—
246	2.4061	—	2.3625	—	2.0257	—	2.3301	—	0.1051	-2.98	0.0101	3.06
276	2.6252	—	2.0897	—	2.0126	—	1.8262	-1.25	2.5987	—	2.2586	—

the roadway can be adjusted, so as to achieve the purpose of optimizing the mine ventilation system.

7 CONCLUSION AND FUTURE DIRECTIONS

To conserve energy and reduce emissions in mines, combined with the mine ventilation law, the total power consumption of the ventilation network was minimized. This was achieved by establishing a mine nonlinear optimization model, which was converted into a non-constrained optimization problem by using the penalty function method and solved using the IEO algorithm. The experimental analysis of the algorithm showed that the convergence speed and accuracy of the algorithm are better than those of other algorithms. The engineering application showed that this method can effectively reduce the fan power by 333 kW, saving more than 2 million yuan RMB per year. This will have a pronounced effect on energy conservation and emission reductions.

With the continuous progress of 5G technology, mine ventilation systems will become more intelligent. In the future, various sensors can be arranged in the branches to collect real-time monitoring data. These data can then be input into intelligent decision-making systems to achieve efficient, energy saving, and safe operation of the mine ventilation system. Furthermore, the optimization of mine ventilation systems is not only related to the efficiency of the main fans but can also be considered by establishing a multi-objective optimization model to determine the largest fan shaft power, the highest efficiency of the main fans, and the smallest total resistance of mine ventilation.

REFERENCES

- Abdel-Basset, M., Mohamed, R., Mirjalili, S., Chakraborty, R. K., and Ryan, M. J. (2020). MOEO-EED: A Multiobjective Equilibrium Optimizer with Exploration-Exploitation Dominance Strategy [J]. *Knowledge-Based Syst.* 214 (6), 106717. doi:10.1016/j.swevo.2020.100791
- Dinh, P.-H. (2021). Multi-modal Medical Image Fusion Based on Equilibrium Optimizer Algorithm and Local Energy Functions. *Appl. Intell.* 51 (11), 8416–8431. doi:10.1007/s10489-021-02282-w
- Dinkar, S. K., Deep, K., Mirjalili, S., and Thapliyal, S. (2021). Opposition-based Laplacian Equilibrium Optimizer with Application in Image Segmentation Using Multilevel Thresholding. *Expert Syst. Appl.* 174, 114766. doi:10.1016/j.eswa.2021.114766
- Dong, M. H., and Li, J. (2008). Analysis on Surging in Axial-Flow Fan and Precautions [J]. *Chin. J. Turbomach.* (4), 66–67. doi:10.3969/j.issn.1006-8155.2008.04.019
- Dorigo, M., Birattari, M., and Stutzle, T. (2006). Ant Colony Optimization. *IEEE Comput. Intell. Mag.* 1 (4), 28–39. doi:10.1109/mci.2006.329691
- Fan, Q., Huang, H., Yang, K., Zhang, S., Yao, L., and Xiong, Q. (2021). A Modified Equilibrium Optimizer Using Opposition-Based Learning and Novel Update Rules. *Expert Syst. Appl.* 170, 114575. doi:10.1016/j.eswa.2021.114575
- Faramarzi, A., Heidarinejad, M., Mirjalili, S., and Gandomi, A. H. (2020b). Marine Predators Algorithm: A Nature-Inspired Metaheuristic. *Expert Syst. Appl.* 152, 113377. doi:10.1016/j.eswa.2020.113377
- Faramarzi, A., Heidarinejad, M., Stephens, B., and Mirjalili, S. (2020a). Equilibrium Optimizer: A Novel Optimization Algorithm. *Knowledge-Based Syst.* 191, 105190. doi:10.1016/j.knsys.2019.105190

DATA AVAILABILITY STATEMENT

The original contributions presented in the study are included in the article/**Supplementary Material**; further inquiries can be directed to the corresponding author.

AUTHOR CONTRIBUTIONS

BY contributed to the conception and design of the study, organized the database, performed the statistical analysis, and wrote the first draft of the manuscript. LS wrote sections of the manuscript. All authors contributed to manuscript revision and have read and approved the submitted version.

FUNDING

The authors disclosed receipt of the following financial support for the research, authorship, and/or publication of this paper: this work was supported by National Natural Science Foundation of China: Research on prediction method and application of coal and gas outburst based on big data (71771111).

SUPPLEMENTARY MATERIAL

The Supplementary Material for this article can be found online at: <https://www.frontiersin.org/articles/10.3389/fenrg.2022.913817/full#supplementary-material>

- Gleiser, R. J., and Dotti, G. (2005). Linear Stability of Einstein-Gauss-Bonnet Static Spacetimes: Vector and Scalar Perturbations. *Phys. Rev. D.* 72 (12), 124002. doi:10.1103/physrevd.72.124002
- Hao, X. H., Wang, Y. Q., and Wang, L. (2012). Application of Transient Chaotic Network Algorithm to Optimization of Mine Ventilation Network[J]. *J. Lanzhou Univ. Tech.* 38 (01), 71–74. doi:10.3969/j.issn.1673-5196.2012.01.017
- Jia, S. P., Wu, G. J., and Chen, W. Z. (2011). Application of Finite Element Inverse Model Based on Improved Particle Swarm Optimization and Mixed Penalty Function[J]. *Rcok Soil Mech.* 32 (S2), 598–603. doi:10.16285/j.rsm.2011.s2.042
- Kaur, S., Awasthi, L. K., Sangal, A. L., and Dhiman, G. (2020). Tunicate Swarm Algorithm: A New Bio-Inspired Based Metaheuristic Paradigm for Global Optimization. *Eng. Appl. Artif. Intell.* 90, 103541. doi:10.1016/j.engappai.2020.103541
- Li, J., Chen, K., and Lin, B. Q. (2007). Genetic Algorithm for Optimization of Mine Ventilation Network[J]. *J. China Univ. Ming Tech.* (06), 789–793. doi:10.3321/j.issn:1000-1964.2007.06.015
- Marini, F., and Walczak, B. (2015). Particle swarm optimization (PSO). A tutorial. *Chemom. Intelligent Laboratory Syst.* 149, 153–165. doi:10.1016/j.chemolab.2015.08.020
- Mirjalili, S. (2016). SCA: a sine cosine algorithm for solving optimization problems. *Knowledge-Based Syst.* 96, 120–133. doi:10.1016/j.knsys.2015.12.022
- Oliveira, M., Bastos-l'illo, C. J. A., and Menezes, R. (2015). Gsing network sci-ence to assess particle swarm Optimizers[J]. *Soc. Netw. Analysis Min.* 5 (1), 1–13. doi:10.1007/s13278-015-0245-5
- Pei, X. D., Wang, K., and Li, X. W. (2017). Analysis and Simulation of Intensive Mine Air Regulation Model Based on The Cellular Automation [J]. *J. China Univ. Ming Tech.* 46 (04), 755–761. doi:10.13247/j.cnki.jcunt.000697

- Peterson, G. Arnold's cat map EB/OL. 2020-11-27.
- Poli, R., Kennedy, J., and Blackwell, T. (2007). Particle swarm optimization. *Swarm Intell.* 1 (1), 33–57. doi:10.1007/s11721-007-0002-0
- Sayed, G. I., Khoriba, G., and Haggag, M. H. (2020). A novel Chaotic Equilibrium Optimizer Algorithm with S-shaped and V-shaped transfer functions for feature selection [J]. *J. Ambient Intell. Humaniz. Comput.*, 1–26. doi:10.1007/s12652-021-03151-7
- Shao, L. S., Wang, Z., and Li, C. M. (2021). Optimization Algorithm of Mine Ventilation Based on SA-IPSO[J]. *J. Syst. Simul.* 33 (09), 2085–2094.
- Shao, L. S., Yu, B. C., and Chen, X. (2020). Key Technique of Mine Intelligent Ventilation[J]. *Saf. Coal Mines* 51 (11), 121–124. doi:10.13347/j.cnki.mkaq.2020.11.025
- Su, S. L., and Ouyang, M. S. (2021). Intelligent Ventilation Management Method of Coal Mine Based on Rough Set and Improved Capsule Network [J/OL]. *Coal Sci. Tech.*, 1–10. [2021-03-10]. doi:10.13199/j.cnki.cst.2021.07.017
- Su, Y. X., Ge, L., and Cheng, S. J. (2017). Mine Ventilation Rate Forecasting Based on Improved Genetic Algorithm and BP neural Network[J]. *J. Henan Polytech. Univ. Nat. Sci.* 36 (4), 20–25. doi:10.16186/j.cnki.1673-9787.2017.04.004
- Wang, B., Wang, Y. S., and Hao, J. B. (2019). Optimization of Intelligent Ventilation System in Wanglou Coal Mine. *J. Saf. Coal Mines* 50 (02), 105–108. doi:10.13347/j.cnki.mkaq.2019.02.024
- Wang, J., Yang, B., Li, D., Zeng, C., Chen, Y., Guo, Z., et al. (2021). Photovoltaic cell parameter estimation based on improved equilibrium optimizer algorithm. *Energy Convers. Manag.* 236 (3), 114051. doi:10.1016/j.enconman.2021.114051
- Wei, G. (2011). Optimization of Mine Ventilation System Based on Bionics Algorithm. *Procedia Eng.* 26, 1614–1619. doi:10.1016/j.proeng.2011.11.2345
- Wu, X. Z., Hu, J. H., and Wei, L. J. (2019). Research on Opposition Based Enhanced Fireworks Algorithm Optimization for Mine Ventilation Network[J]. *Industry Mine Automation* 45 (10), 17–22. 67. doi:10.13272/j.issn.1671-251x.17438
- Zhang, X. G., and Zhou, Y. (2018). Study on ACPSO algorithm for mine ventilation Network[J]. *J. Liaoning Tech. Univ. Sci. Ed.* 20 (04), 305–311.
- Zhong, D., Wang, L., Wang, J., and Jia, M. (2020). An Efficient Mine Ventilation Solution Method Based on Minimum Independent Closed Loops. *Energies* 13 (22), 5862. doi:10.3390/en13225862

Conflict of Interest: The authors declare that the research was conducted in the absence of any commercial or financial relationships that could be construed as a potential conflict of interest.

Publisher's Note: All claims expressed in this article are solely those of the authors and do not necessarily represent those of their affiliated organizations, or those of the publisher, the editors and the reviewers. Any product that may be evaluated in this article, or claim that may be made by its manufacturer, is not guaranteed or endorsed by the publisher.

Copyright © 2022 Yu and Shao. This is an open-access article distributed under the terms of the Creative Commons Attribution License (CC BY). The use, distribution or reproduction in other forums is permitted, provided the original author(s) and the copyright owner(s) are credited and that the original publication in this journal is cited, in accordance with accepted academic practice. No use, distribution or reproduction is permitted which does not comply with these terms.